Oxidation of Pt(110)

W. X. Li,[1] L. Österlund,[1,2] E. K. Vestergaard,[1] R. T. Vang,[1] J. Matthiesen,[1] T. M. Pedersen,[1] E. Lægsgaard,[1]
B. Hammer,[1] and F. Besenbacher[1]

[1]*Interdisciplinary Nanoscience Center (iNANO), Center for Atomic-scale Materials Physics (CAMP),
and Department of Physics and Astronomy, University of Aarhus, DK 8000 Aarhus C, Denmark*
[2]*Department of Environment and Protection, FOI NBC Defense, SE 901 82 Umeå, Sweden*
(Received 4 March 2004; published 29 September 2004)

Using scanning tunneling microscopy and temperature programed desorption we investigate the
Pt(110) surface under strongly oxidizing conditions involving either high-pressure O_2 or atomic oxygen
exposure. At low temperatures, only disordered Pt oxide structures are observed. After annealing
ordered surface oxide islands are observed to coexist with a highly stable reconstructed (12×2)-O
chemisorption structure. From density functional theory calculations a model for the surface oxide
phase is revealed. The phase is found to be metastable, and its presence is explained in terms of
stabilizing defects in the chemisorption layer and reduced Pt mobility.

Oxide formation on transition metal (TM) surfaces is important in many disciplines including surface coatings in materials science and supported metal particles in heterogeneous catalysis. Considerable advances have recently been made in the microscopic understanding of oxide formation on TM surfaces [1–4]. Knowledge of the microscopic state of a metal surface is essential for a description of physiochemical processes at the surface. For instance, a catalytic oxidation reaction may proceed completely differently over a metallic surface (e.g., via a Langmuir-Hinshelwood mechanism) as compared to over an oxide surface (e.g., via a Mars-van Krevelen mechanism)[5]. So far, most studies have focused on the close-packed $4d$ TM surfaces. Depending on the TM, either bulk or surface oxides are formed under high O_2 pressures. To the right in the transition metal series, the oxide formation becomes thermodynamically less favored, and in some cases, the substantial reconstructions associated with the formation of the oxides have been found to set up kinetic restrictions [6,7].

Many open questions remain in the field, including differences between the $4d$ and other TM elements, as well as between open- and close-packed surfaces. To address these issues, we present here a combined experimental and theoretical investigation of the oxide formation on an open $5d$ TM element, Pt(110). Platinum is chosen since it is one of the technologically most important catalysts, used, e.g., for emission cleaning, and its oxide, PtO_2, is a well-known hydrogenation catalyst. Previous ultrahigh vacuum (UHV) studies have shown that the Pt(110) surface exhibits a variety of surface structures upon O_2 exposures [8,9]. Recently, a disordered phase was reported to develop on Pt(110) under O_2 rich conditions during CO oxidation, and this was interpreted as being due to oxide formation [10]. In this Letter we reveal, by an interplay between scanning tunneling microscopy (STM) and temperature programed desorption (TPD) experiments and density functional theory (DFT)

calculations, the atomic-scale structure of high-coverage oxygen structures on the Pt(110) surface, including the formation of platinum oxide. Furthermore, we determine under what conditions the oxide exists. The experimental setup is described elsewhere [11,12]. High-pressure O_2 exposures were made in a dedicated high-pressure cell, and a thermal gas cracker source was employed for atomic O dosing at UHV compatible pressures.

When Pt(110) is exposed at room temperature (RT) to either atomic O under UHV conditions [Fig. 1(a)] or to high pressures of O_2 (inset), a disordered overlayer structure develops. The structure exhibits weak ordering along the $[1\bar{1}0]$ direction at low O exposures, with the Pt(110)-(1×2) structure discernible underneath. With increasing O exposures, all traces of the original surface structure are, however, erased.

New, ordered structures are observed after brief annealing or when O exposure is performed at elevated temperatures. Dosing O at 500 K [Fig. 1(b)] results in two surface phases. Guided by previous studies and by our TPD and DFT results below, one of the phases, which consists of $[1\bar{1}0]$-oriented stripes aligned along the [001] direction, is concluded to be the saturation of the O chemisorption phase [8,9]. The other phase consists of a novel island structure, which is discussed in detail below. When dosing at even higher temperatures, 600 K [Fig. 1(d)], only the chemisorption phase remains. High-resolution images [Fig. 1(d), bottom left] unambiguously show that this is a structure built from $(n \times 2)$ units, where n is very narrowly peaked around 12, henceforth denoted (12×2) structure. Each (12×2) repeat unit contains a stripe with ten distinct protrusions separated by ~ 4 Å wide and ~ 0.5 Å deep depressions. These depressions are deeper and more narrow than those observed in the domain structures found at lower O coverage, where the Pt(110) surface remains intact [8,9], and the depressions are accordingly assigned to vacancies, where two Pt atoms have been pushed out between

neighboring stripes [13]. The remaining Pt atoms are expanded $\sim 14\%$ in the $[1\bar{1}0]$ direction, and our DFT modeling indicates a strong adsorption of 22 O atoms per stripe [14]. A similar (10×2) O structure has been observed on Rh(110) [15].

STM imaging of the small islands that appear after O exposure at 500 K [Fig. 1(c)] or following high-pressure O_2 exposures at 355 K is possible only at bias voltages ≥ 1 V, indicating that the electronic structure of the islands is associated with a band gap. It is therefore reasonable to associate these islands with patches of surface oxide phase. Our calculations below further substantiate this assignment. The oxide islands appear to consist of stripes similar to those in the (12×2) structure with a similar expansion along $[1\bar{1}0]$. The stripes are, however, shifted
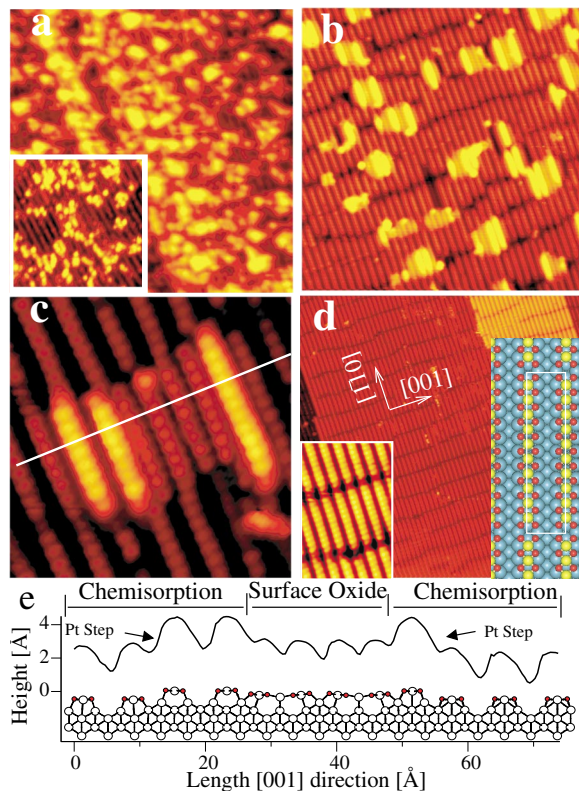
FIG. 1 (color). STM images of the Pt(110) surface after exposure to (a) 5 min atomic O at 298 K $(300 \times 300$ Å$^2)$. Inset: 0.01 mbar O_2 for 10 min at 355 K $(150 \times 150$ Å$^2)$. (b) 60 min atomic O at 500 K $(300 \times 300$ Å$^2)$. (c) 60 min atomic O at 500 K. High-resolution image $(60 \times 60$ Å$^2)$ of surface oxide island. The middle part of the island reveals a surface oxide while the protruding stripes are second layer Pt rows with chemisorbed O. (d) 75 min atomic O at 600 K $(500 \times 500$ Å$^2)$. Insets: high-resolution image $(46 \times 77$ Å$^2)$ of the chemisorption phase and associated ball model of the (12×2)-22 O chemisorption structure. (e) A line scan along the white line in (c) and a ball model based on the DFT calculations presented below. All STM measurements were made in UHV at 298 K with $I = 1.5$–2 nA, $V = 1$–1.75 V.

by half a Pt-Pt separation in the $[1\bar{1}0]$ direction. Within the islands, some stripes protrude higher (~ 1.4 Å) compared to the other stripes in the islands (~ 0.4 Å) [Fig. 1(e)] with respect to the (12×2) structure. These stripes are typically found at the [001] edges of the islands, but in a few cases also inside the islands, proving that the brightness is not a result of an electronic edge state. Moreover, they are always shifted $\pm 1/4$ of the (12×2) cell in the [001] direction. These stripes are therefore attributed to second layer Pt rows with chemisorbed O atoms. For the less protruding stripes within the islands, a 29% compression in the [001] direction is observed. The projected surface area covered by islands ($\sim 16\%$) at 500 K corresponds well to the amount of Pt removed from the lattice to form the (12×2) superstructure (2 out of 12 Pt atoms) and indicates that the surface oxide islands are formed by rearrangement of such Pt atoms. The surface containing only the chemisorption phase after deposition at 600 K appears smoother with larger terraces than the clean Pt(110) surface, which typically exhibits a periodic buckling along the [001] direction with a high step density along $[1\bar{1}0]$ [16]. This indicates that the Pt atoms from the formation of vacancies between the stripes are mobile at 600 K and bind to the step edges instead of forming surface oxide islands.

Figure 2 shows TPD spectra obtained after atomic O and O_2 exposures (all O desorbs associatively as O_2). The peak at 730 K (β_4) with the high temperature shoulder at ~ 800 K (β_5) is associated with O_2 desorbing from the (12×2) structure and defect sites, respectively [9]. TPD spectra obtained after O exposure at 600 K confirmed this. In such spectra [Fig. 2(b), dashed line] only the β_4 and β_5 peaks are revealed, which corresponds to the STM images [Fig. 1(d)] exhibiting only the (12×2) chemisorption structure. The β_4 peak is accordingly used for absolute coverage calibration [corresponding to $22/12 = 1.83$ ML (monolayer)]. The β_4 peak is stronger than the
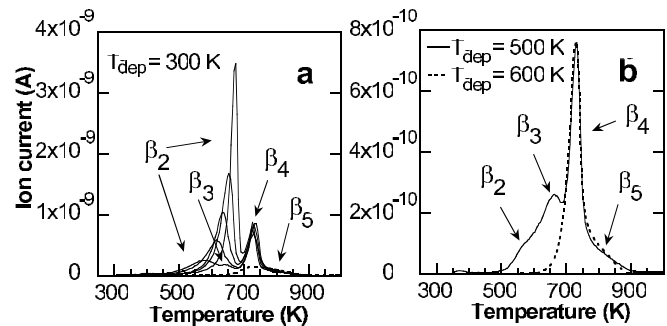
FIG. 2. (a) TPD spectra of O_2 obtained after 5 to 20 min atomic O exposures at 300 K, corresponding to 4.4, 5.0, 5.7, 7.3, and 8.7 ML, as well as after 500 L O_2 exposure (1.2 ML, dashed line). An additional weak peak (β_1) appears at ~ 400 K at the highest exposures (not shown). (b) TPD spectra obtained after atomic O exposure at 500 and 600 K, respectively. Heating rate: 2.5 K/s.

corresponding TPD peak obtained after low-pressure O_2 exposures (500 L, dashed line in Fig. 2(a)] due to the completion of the (12×2) structure. A prominent TPD peak (β_2) builds up at 560 K and shifts to 680 K after 20 min atomic O exposure at 300 K and is the main TPD peak at high O exposures, where the integrated area shows an O uptake corresponding to 8.7 monolayer. Such high O coverages clearly indicate that bulk oxides are formed upon extended O exposure at RT conditions. Similar TPD spectra have been reported for O_3/Pt(111) [17]. The β_2 peak is substantially reduced or absent after O exposure at 500 and 600 K, respectively [Fig. 2(b)]. After dosing at 500 K, a peak at 650 K (β_3) is clearly visible. Since this TPD peak correlates with the presence of the islands observed in Figs. 1(b) and 1(c), we assign β_3 to the decomposition of these islands.

We start the account of our DFT calculations [18] by addressing the (12×2) structure. On Pt(110)(1×2) oxygen adsorbs in fcc sites along the Pt ridge causing a build up of stress [8]. From the presented STM images we found that the stress is relieved by a $\sim 14\%$ expansion of the Pt-Pt interatomic distance along the $[1\bar{1}0]$ direction on the ridges. In order to describe this with an affordable computational scheme, we focus on the middle (1×2) section of the structure and expand the whole Pt(110) by 14% in the $[1\bar{1}0]$ direction prior to the introduction of oxygen [19]. The resulting chemisorption structure [Fig. 3(a)] has a formation energy/O atom with respect to $O_2(g)$, ΔE_O, which is -1.57 eV [Fig. 4(a)].

The formation energies of the three bulk Pt oxides, PtO, α-PtO$_2$, and β-PtO$_2$, are calculated to be $\Delta E_O = -0.41$, -0.62, and -0.64 eV per O, respectively, in agreement with experimental evidence of α and β-PtO$_2$ being the most stable oxides with a formation energy of -0.69 eV [20]. Inspired by the compressed islands in Fig. 1(c), we have calculated the structure and stability of the chemisorption structure compressed by 20%, 25%,

and 33% in the [001] direction [Figs. 3(b)–3(d)]. The structure compressed by 20% [Fig. 3(b)] takes the form of a β-PtO$_2$(110) surface (strained -0.8% and $+2.5\%$ in the in-plane directions) stripped from weakly bound bridging O. The structures compressed 25% and 33% are both very stable. The former [Fig. 3(c)] has no bulk oxide analog, while the latter [Fig. 3(d)] adopts the form of the PtO(100) surface, strained -2.0% and $+2.5\%$ in plane. The Pt density in the structure of Fig. 3(d) is the same as in the α-PtO$_2$(0001) surface (when strained -1.7% and $+3.0\%$ in plane) meaning that the addition of O atoms would lead to a single (tri-)layer structure of the α-PtO$_2$ [Fig. 3(e)] without long-range Pt rearrangement. Second layers of the β and α-PtO$_2$ oxides can be added [Figs. 3(f) and 3(g)], whereby the average O binding approaches the formation energy of the bulk oxides [Fig. 4(a)].

To investigate the expected state of the surface under varying oxidation conditions we turn to the formation *free* energy per (1×2) unit area, $\Delta G = (\Delta E_O - \Delta \mu_O) \times n_O$, where $\Delta \mu_O$ is the change in the chemical potential of oxygen due to temperature and pressure, and n_O is the number of O atoms in the (strained) (1×2) cell [4,21]. From ΔG it is clear [Fig. 4(b)] that in the thermodynamic limit, our calculations predict the formation of bulk oxide for $\Delta \mu_O > -0.64$ eV and the formation of the 2 ML chemisorption structure at lower $\Delta \mu_O$'s. The surface oxide structures are metastable and must be stabilized, e.g., by defects and/or kinetic restrictions. Referring to Fig. 1(b), we note that the surface oxide islands are indeed found in conjunction with imperfections in the (12×2) structure. Furthermore, the surface oxide islands are found only at temperatures, 500 K, where Pt diffusion to the step edges (as seen at 600 K) is suppressed, meaning that Pt atoms ejected from the ridges are locally available at an energetically lower cost than Pt atoms from the bulk reservoir.
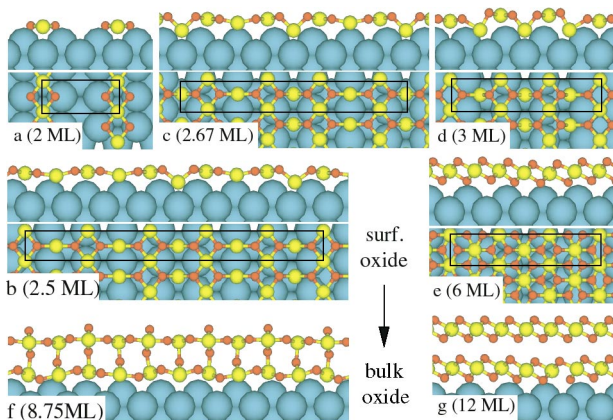
FIG. 3 (color). Ball-and-stick models of (a) the chemisorption, (b)–(e) surface oxide, and (f),(g) thicker oxide structures modeled with DFT. Red, yellow, and blue spheres: oxygen, oxidic, and metallic platinum atoms.
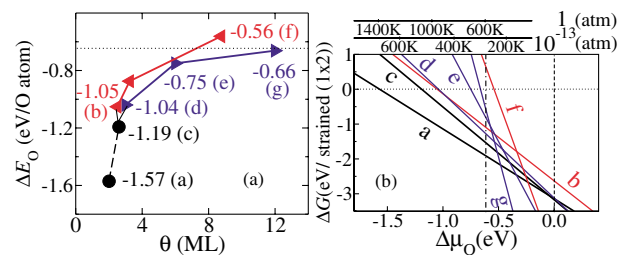
FIG. 4 (color). (a) The formation energy per O atom, ΔE_O, as a function of O coverage. Extra Pt atoms are taken from bulk reservoirs. (b) Formation free energy per (strained) surface (1×2) area with respect to $\Delta \mu_O$. The reference point (dotted vertical line) is $\mu_O = 1/2 E_{O_2}$, while the dot-dashed vertical line corresponds to the heat of formation of α-PtO$_2$. Temperature scales at two typical pressures of O_2 have been indicated.

In constructing the model of an oxide island in Fig. 1(e), we have used the surface oxide structure of Fig. 3(c) since this structure has a low ΔG at high temperatures and a compression (25%) close to the measured (29%). The assignment of the β_3 TPD peak to the surface oxide islands is now further corroborated by (i) the qualitative finding that the structure of Fig. 3(c) does not support bulk oxide growth, explaining why the peak neither grows nor shifts with O uptake, and by (ii) the quantitative finding of 0.5 ± 0.1 ML O in the β_3 peak. With a 16% island coverage this implies a local O coverage of 3.1 ± 0.6 ML within the islands, which compares well with the 2.67 ML in the structure of Fig. 3(c).

In contrast to the β_3 peak, the β_2 peak grows with increasing O coverage and shifts to higher temperatures. We already assigned this peak to oxide growth on experimental grounds, and from the DFT results we see that both the α-PtO$_2$ and the β-PtO$_2$ phase are candidates for the 3D oxide structure. The crossing in Fig. 2 of the leading edges of the β_2 peaks indicates an increasing barrier for decomposition with increasing O uptake. This is consistent with an increasing differential binding energy (the energy required to remove the *first* O atom) for which we, e.g., calculate 1.04 eV for the α-PtO$_2$ surface oxide [Fig. 3(e)], and 1.79 eV for the thicker oxide [Fig. 3(g)], further supporting our assignment of the β_2 peak to bulk oxide growth.

To place our findings in a general context, we note that in order to form a stable surface oxide, the chemisorption phase and the surface oxide phase must coexist (their ΔG's must cross) at a $\Delta\mu_O$ for which the bulk oxide has not formed yet. To split the effect of studying $4d$ vs $5d$ and dense vs open surfaces, we have performed calculations for the Pd(110) surface assuming similar chemisorption [Fig. 3(a)] and surface oxide [Fig. 3(c)] structures as for Pt(110). A major difference between the $4d$ and $5d$ TMs is the cohesive energy which is systematically larger for the $5d$ TMs (e.g., 3.89 eV for Pd and 5.84 eV for Pt). In our calculations, the cohesive energy enters the surface oxide formation energies (since metal atoms are taken from the bulk reservoir), while it does not enter the chemisorption energies. Yet, comparing Pd(110) and Pt(110), we calculate very similar energetics (on Pd, the chemisorption and surface oxide phases are only 0.27 and 0.32 eV/O weaker than on Pt) meaning that the great difference in cohesive energies is compensated by an enhanced metal-oxygen binding for the Pt system. This rationale also explains the similar oxide formation energies for PdO and PtO$_2$ (experimentally: -0.88 and -0.69 eV/O at standard conditions).

We thus attribute the finding of the only metastable surface oxides on Pt(110) and Pd(110) to the openness of these surfaces, which allows for a particularly (numerically) high ΔG for the chemisorption phase. In fact, at, for example, $\Delta\mu_O = -0.4$ eV (corresponding $\sim$417 K at 1 atm), we calculate a ΔG of -91 meV/Å^2 and -70 meV/Å^2 for the chemisorption phases over Pt(110) and Pd(110) which is to be compared to -67 meV/Å^2, -39 meV/Å^2, -24 meV/Å^2, and -6 meV/Å^2 for Rh(111) [7], Pd(111) [2], Pd(100) [6], and Ag(111) [4] at 0.25 ML, the latter three systems (with small ΔG's) all having stable surface oxides. The favorable chemisorption of oxygen in every fcc site on either side of the close-packed ridge of the (110) surface is responsible for the (numerically) large ΔG, which in turn leaves little room for an improved binding in a surface oxide, thereby moving the point of phase coexistence far into the region of a stable bulk oxide.

[1] H. Over *et al.*, Science **287**, 1474 (2000).
[2] E. Lundgren *et al.*, Phys. Rev. Lett. **88**, 246103 (2002).
[3] C. I. Carlisle *et al.*, Phys. Rev. Lett. **84**, 3899 (2000).
[4] W. X. Li *et al.*, Phys. Rev. Lett. **90**, 256102 (2003).
[5] C. Doornkamp and V. Ponec, J. Mol. Catal. A **162**, 19 (2000).
[6] E. Lundgren *et al.*, Phys. Rev. Lett. **92**, 046101 (2004).
[7] J. Gustafson *et al.*, Phys. Rev. Lett. **92**, 126102 (2004).
[8] S. Helveg *et al.*, Surf. Sci. **430**, 533 (1999).
[9] A. V. Walker and D. A. King, J. Chem. Phys. **109**, 6879 (1998).
[10] B. L. M. Hendriksen and J. W. M. Frenken, Phys. Rev. Lett. **89**, 046101 (2002).
[11] L. Österlund *et al.*, Phys. Rev. Lett. **86**, 460 (2001).
[12] E. Lægsgaard *et al.*, Rev. Sci. Instrum. **72**, 3537 (2001).
[13] In the oxygen structures studied by Helveg *et al.* no Pt atoms where pushed out from the close-packed ridges.
[14] O binds differentially with 1.76 eV (1.59 eV) at middle (terminal) positions in the (12 × 2)-22 O structure, as estimated from calculations using (6 × 2) cells.
[15] E. Vesselli *et al.*, J. Chem. Phys. **114**, 4221 (2001).
[16] T. Gritsch *et al.*, Surf. Sci. **257**, 297 (1991).
[17] N. A. Saliba *et al.*, Surf. Sci. **419**, 79 (1999).
[18] Perdew-Wang 91 exchange correlation, ultrasoft pseudopotentials, and plane waves cut off at 25 Ry are used. The slabs consist of five atomic layers of Pt(110), three of them fully relaxed, supporting O on one side. $(8 \times 8/N)$ **k**-point grids are used for surface Brillouin zone sampling for $(1 \times N)$, $N = 2, 4, 8$ surface cells.
[19] The present model with 2 ML per strained (1×2) Pt(110) unit shows differential O binding of 1.72 eV close to the values obtained when including mismatch between the Pt ridge and the Pt(110) [14].
[20] *The Oxide Handbook*, edited by G. V. Samsonov (IFI/Plenum, New York, 1973).
[21] K. Reuter and M. Scheffler, Phys. Rev. B **65**, 035406 (2002).